Relationship between Self-Association of Glycine Molecules in Supersaturated Solutions and Solid State Outcome

Deniz Erdemir,[1] Soma Chattopadhyay,[2,3] Liang Guo,[4,2] Jan Ilavsky,[5] Heinz Amenitsch,[6] Carlo U. Segre,[2] and Allan S. Myerson[1]

[1]*Department of Chemical Engineering, Illinois Institute of Technology, Chicago, Illinois 60616, USA*
[2]*CSRRI and BCPS Department, Illinois Institute of Technology, Chicago, Illinois 60616, USA*
[3]*MRCAT, Building 433B, Advanced Photon Source, 9700 South Cass Avenue, Argonne, Illinois 60439, USA*
[4]*BioCAT, Building 435B, Advanced Photon Source, 9700 South Cass Avenue, Argonne, Illinois 60439, USA*
[5]*Argonne National Laboratory, 9700 South Cass Avenue, Argonne, Illinois 60439, USA*
[6]*Institute of Biophysics and Nanosystems Research, Austrian Academy of Sciences, Schmiedlstrasse 6, A8042, Graz, Austria*

(Received 18 October 2006; published 13 September 2007)

Small angle x-ray scattering is utilized to directly examine the formation of clusters in supersaturated solutions of glycine, in an attempt to understand their role in the nucleation process. The results suggest that the majority of glycine molecules exist as dimers in aqueous solutions, and monomers in 13% (v/v) acetic acid-water mixtures. As the water and acetic acid–water solutions crystallize into α and γ forms, respectively, the findings indicate a direct correlation between molecular self-association in solution and the polymorphic outcome.

DOI: 10.1103/PhysRevLett.99.115702 PACS numbers: 64.60.Qb, 64.60.My, 64.90.+b

Solution crystallization is vital to many processes occurring in nature. The initial stage of crystallization—the period between the achievement of supersaturation and the formation of nuclei—is crucial in determining the final product properties. Classical nucleation theory (CNT), which allows estimation of the critical size and nucleation rate, provides no information regarding the pathways leading from the solution to the solid crystal and may not even be qualitatively correct [1]. Theoretical and experimental studies suggest that nucleation from supersaturated solutions might be a two-step process, where density fluctuations occur prior to structure fluctuations [2–6]. A recent small angle x-ray scattering (SAXS) study by our group demonstrated that glycine dimers in supersaturated solutions transform from mass fractal to surface fractal structures prior to nucleation, suggesting that the formation of a liquidlike critical cluster is followed by organization into a lattice, as opposed to the CNT where the fluctuations in density and structure order parameters proceed simultaneously [7]. Even though numerous experimental studies have reported the existence of prenucleation clusters in supersaturated solutions of small molecules, most of these studies do not provide direct evidence about the structure of the clusters or their influence on the solid state outcomes [8,9]. The growth of a desired polymorph can be promoted by additives that selectively inhibit the undesired structures, based on the hypothesis that supersaturated solutions contain clusters with packings corresponding to all the polymorphs of a system [10–12]. Recently, the nature of the solute-solvent interactions was shown to significantly affect the initial association of solute molecules and the polymorphic outcome of the crystallization, providing evidence for a direct link between molecular self-association in solution and the crystallized solid form [13–15].

In the present study, SAXS is utilized to directly measure the formation and evolution of prenucleation clusters in supersaturated solutions of glycine, in order to understand the relationship between self-assembly of solute molecules and the final crystal structure, and ultimately develop a structural perspective of the nucleation process. Glycine is known to exist as a zwitterion ($^{+}H_3N\text{-}CH_2\text{-}COO^{-}$) in aqueous solution at the isoelectric point (pH 6.2). The existence of zwitterions strongly depends on the solution pH, as the carboxyl group is protonated to give cations ($^{+}H_3N\text{-}CH_2\text{-}COOH$) at pH values below 2.35, while the amino group is deprotonated to give anions ($H_2N\text{-}CH_2\text{-}COO^{-}$) at pH values above 9.78 [16]. Glycine has three crystalline modifications under ambient conditions, the α, β, and γ forms whose order of thermodynamic stability is $\gamma > \alpha > \beta$ [17]. The crystal lattice of α glycine is composed of centrosymmetric double layers that are held firmly intact by hydrogen bonds between cyclic molecular pairs and crystallizes spontaneously from aqueous solutions with bipyramidal morphology [18]. In the crystal lattice of γ glycine, molecules are arranged in helical chains around the threefold screw axes parallel to the c axis and packed into a three-dimensional network by lateral hydrogen bonds [19]. γ glycine crystallizes from aqueous solutions made acidic with acetic acid or sulfuric acid, or basic with ammonium-hydroxide [19].

SAXS measurements were performed at the BioCAT beam line (18-ID) at the Advanced Photon Source, Argonne National Laboratory. Glycine solutions at concentrations ranging from 3.60 to 4.27 M were prepared by combining solid glycine, 99.8% (Sigma), and deionized water ($\rho = 18\ \mathrm{M\Omega\,cm}$) in test tubes and heating in an ultrasonic water bath at 60 °C until the glycine was com-

pletely dissolved. Half of these solutions were made acidic (pH ~ 3.6) by further addition of glacial acetic acid (Pharmco Products Inc.), at 13% by volume. Solution samples of ~ 100 μl were loaded into thin-walled glass capillaries of diameter 2 mm, sealed, and placed vertically in a brass sample holder, which was fitted to a PE120 Peltier heating/cooling stage (Linkam Scientific Instruments) and aligned with the beam. The temperature of the stage was controlled remotely and the actual temperature was recorded from a thermocouple inserted into a small cavity close to the capillary. Data collection was started immediately with the temperature of the sample holder being reduced from 65 to 6.5 °C at the rate of 4 °C/ min, in order to achieve supersaturation. The saturated aqueous solution of glycine has a concentration of 2 M at 65 °C, which allowed measurements at supersaturation (SS) levels ranging from 1.8 to 2.1 following the cooling period (SS $= c/c_o$, where c is the actual concentration and c_o is the saturation concentration). Even though the addition of acetic acid dilutes the solutions, the degree of supersaturation is expected to be close for the pure and acidic solutions since acetic acid slightly decreases the solubility of glycine (c_o was measured to be 2.8 and 2.6 M at 24 °C in aqueous and acidic solutions, respectively). The SAXS data were collected with x-ray exposures of 20 s at intervals of 60 s until crystallization was observed visually. Since the local heating caused by absorption of x rays decreases the supersaturation, consequently hindering the nucleation process [7], high energy x rays of 25 keV were used to diminish the absorption effects and reduce the induction time to a few hours. The beam size on the sample was 300 μm $\times$ 300 μm and the CCD detector (86 mm $\times$ 49 mm) was placed at 3.23 m from the sample to cover a q range of 0.008 to 0.3 Å^{-1}. Data reduction was performed in Igor Pro (Wavemetrics, Inc.) with macros developed by the BioCAT staff. The scattering profiles were normalized with the transmitted beam intensity measured by a p-i-n diode in the beamstop. The background scattering measured from capillaries filled with water or 13% (v/v) acetic acid-water mixture was removed from the final scattering data. The data were modeled using the Irena package [20].

Crystallization was achieved within two hours in the majority of samples. The aqueous glycine solutions formed multiple bipyramidal-shaped crystals, while needle-shaped crystals were grown vertically along the length of the capillaries in the presence of acetic acid. The crystals were characterized by Raman spectroscopy following the SAXS measurements without being removed from the solutions and α and γ glycine were observed in the pure and acidic solutions, respectively. Guinier analysis was performed in the q range between 0.029–0.30 Å^{-1}, and representative fits are shown in Fig. 1. In spite of the fairly high solution concentrations, the effect of interference between x rays scattered by individual particles was not apparent in the scattering profiles of glycine in acid-free

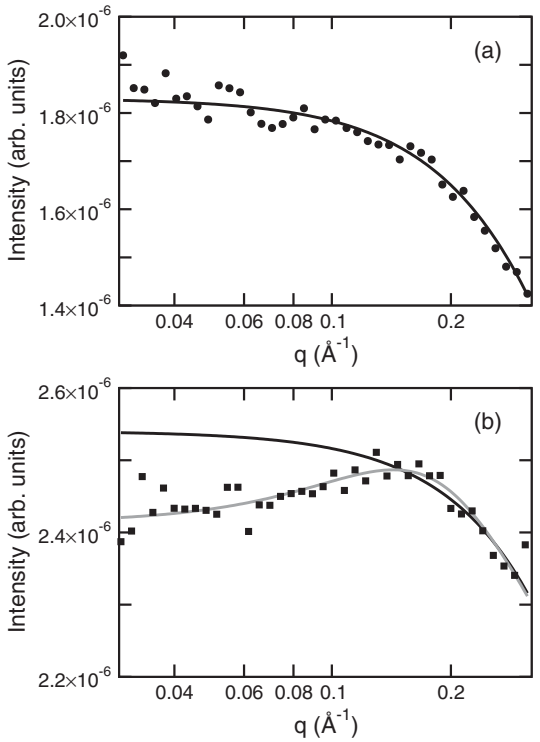

FIG. 1. Guinier fits performed on scattering profiles of (a) 4.05 M pure and (b) 3.61 M acidic glycine solutions at $t =$ 6.5 min, showing experimental data (circles and squares) and Guinier fit with (gray line) and without (black line) interference term.

solutions in this q range [Fig. 1(a)]. However, interparticle interactions were observed in the presence of acetic acid, as manifested by a depressed scattering intensity in the low q region, leading to a local peak in the SAXS curve [Fig. 1(b)]. The SAXS intensity for correlated systems is given by $I(q) = NP(q)S(q)$, where N is the number density of particles, $P(q)$ is the particle form factor, and $S(q)$ is the solution structure factor, which accounts for the interaction of particles in the solution. The scattering profiles without particle interaction were obtained by dividing the experimental intensity by the solution structure factor:

$$S(q) = \frac{1}{1 + pF(q, d)}, \tag{1}$$

where p is the packing density, equal to 8 times the ratio of the hard sphere volume per average volume available. $F(q, d)$ is the form factor function for structural correlation occurring between particles at average radial interparticle distance, d proposed by Beaucage *et al.* [21] for spherically symmetric particles, based on the Born-Green theory. The parameters p and d were determined by fitting the $F(q, d)$ function to the experimental data simultaneously with the Guinier analysis. As expected, the R_g values for the acid-free solutions were independent of the inclusion of the interaction term in the analysis, confirming that $S(q) \sim 1$ for this system.

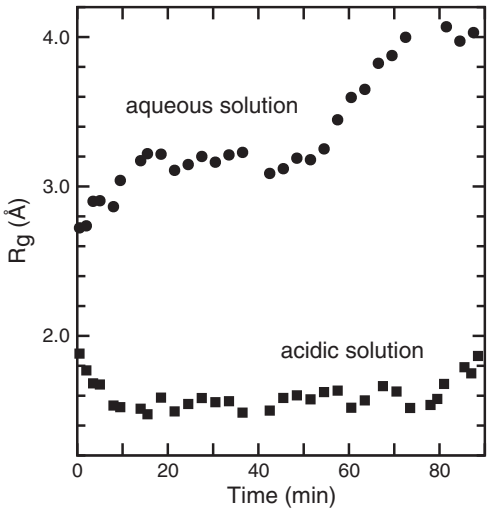

FIG. 2. Variation in radius of gyration over time for 4.05 M pure (circles), and 3.61 M acidic (squares) glycine solutions. The standard deviation of fit values falls within in the symbol size.

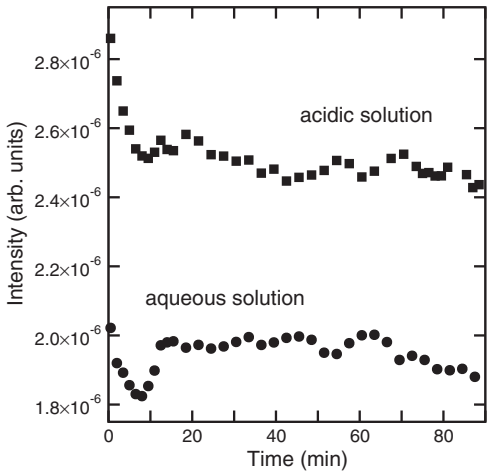

FIG. 3. Variation in intensity over time for 4.05 M pure (circles), and 3.61 M acidic (squares) glycine solutions. Intensities are obtained from Guinier prefactor, $G = NV^2(\Delta\rho)^2$, where N is the number density of particles, V is the particle volume, and $\Delta\rho$ is the electron density difference between particles and solution medium.

Figure 2 shows the variation in radius of gyration (R_g) over time for 4.05 M aqueous glycine solution and 3.61 M acidic glycine solution. The first 15 min corresponds to the cooling period, where the temperature of the solutions was reduced from 65 to 6.5 °C at a constant rate of 4 °C/ min. These trends were reproducible within an error of ± 0.2 Å for four different samples, with slightly different induction times. In the pure glycine solution, R_g monotonically increases from 2.72 to 3.20 Å during the initial 15 min of cooling and then stays near 3.2 Å for the next 40 min at the stabilized temperature of 65 °C. While the radius of the glycine molecule is reported as 2.8 Å, the radius of gyration, which is the root mean square of distances from the center of mass, is expected to be a more compact value, in the range of 1.5–2.0 [22]. Consequently, the initial R_g of 2.7 Å suggests the presence of dimers and even multimers coexisting with monomers before supersaturation is achieved. The increase of R_g to 3.2 Å during the cooling period can be attributed to the progressive dimerization of glycine molecules and formation of multimers with increasing level of supersaturation. The corresponding scattering intensity profile shows an initial decrease, followed by an increase (Fig. 3). These changes occur in a wide low- to mid-q range so they are not likely due to interference effects or large aggregate scattering. Although the cause of the initial decrease in scattering intensity is unclear at the present time, the subsequent increase can be attributed to the increase in the particle volume due to dimerization and possible multimer formation. These results are consistent with the indirect measurements and theoretical studies that reported the existence of dimers in aqueous glycine solutions and the growth of α glycine by assembly of cyclic dimers [9,23,24]. The second increase in R_g at 55 min, which was not observed in samples that did not crystallize, is attributed to the onset of nucleation. It is possible that the dimers and multimers localized in high density domains organize themselves into larger aggregates, leading to the formation of crystals, as proposed in our previous report [7]. The decrease in scattering intensity at 62 min is likely an indication of concentration decrease in the parent solution due to the growth of crystals, which are too large to be detectable in the measured q range. The lag of 7 min between the onset of R_g increase and the onset of scattering intensity decrease is the time needed for reorganization to form crystals. As R_g reaches ~4 Å, the increase in particle size slows down, which may indicate that small nuclei of ~4 Å associate and develop into larger crystals in a very short time span.

In the presence of acetic acid, the R_g and intensity profiles (Figs. 2 and 3, square symbols) display trends differing from those in acid-free solutions, indicating different solution chemistry. It should be noted that the R_g values are approaching the measurable limit (~ 1.3 Å) in the currently probed q range and hence further measurements at higher q are needed to support these data. The small R_g values over the whole process imply that glycine molecules mostly exist as monomers in the 13% (v/v) acetic acid-water mixtures. The decrease from the initial R_g value during the cooling period can be interpreted as the consequence of molecular shrinking due to reduced solubility at the lowered temperatures. The lack of increase in the corresponding scattering intensity over the whole process supports the hypothesis that dimerization is not favorable in the presence of acetic acid, resulting in monomer-rich supersaturated solutions. The inhibition of dimer formation has been suggested in the literature to explain the preferred crystallization of γ glycine in acidic conditions and attributed to the increased concentration of positively charged glycine molecules, which are incapable of forming

cyclic dimers due to repulsion of like charges [12,16]. However, the concentration of cations at $p\mathrm{H} = 3.6$ in our solutions would be too small (5.3% of the total glycine molecules, calculated from pKa_1) to have a significant impact on dimer formation, as has also been stated in a recent study by Towler *et al.* [25]. In addition to the pH effect, the interaction of undissociated acetic acid molecules and acetate ions with glycine zwitterions may play a role in determining the relative proportion of monomers and dimers in the solution. The correlations between particles are expected to be stronger in a solution rich in cations and zwitterions compared to a system of nonpolar cyclic dimers with lower number density. This may explain why interference effects are prominent in the scattering profiles of the acidic glycine solutions. The scattering curve at low q becomes more depressed and the calculated packing density (p) progressively increases during the cooling period, which can be an indication of high density domains, such as liquidlike clusters, evolving with increasing supersaturation. The CCD image at 88 min contains two long intense scattering streaks radiating from the vertically aligned, needlelike crystals. Hence, the observed increase in R_g at $\sim$80 min may correspond to the onset of nucleation.

It has been suggested in earlier studies that molecular cluster formation in glycine solutions increases steadily with concentration [26,27]. Our measured average R_g values prior to the cooling process were 2.92, 2.91, 2.66, and 2.59 Å for 3.60, 3.83, 4.05, and 4.27 M aqueous glycine solutions, respectively. Similarly, the average initial R_g values were 2.21, 1.95, and 1.72 Å for 3.41, 3.61, and 3.81 M acidic glycine solutions, respectively. While the R_g values changed during the course of each experiment, the descending magnitude of R_g with increasing concentration was universal. These results are apparently in contradiction with the notion that glycine has a greater tendency to associate in more concentrated solutions, however, the increased concentration also can lead to a depression of the measured R_g due to stronger interference effects in the scattered x rays.

The observed existence of dimers in aqueous solutions is consistent with the nucleation of α form, which has a double layer structure composed of cyclic dimers. This supports the hypothesis that the tendency for cyclic dimer formation is a factor in the preferred crystallization of α glycine from aqueous solution. Conversely, the scattering data imply that acetic acid-water mixtures are rich in glycine monomers and crystallize into the γ form with a polar chain structure built of monomeric growth units. These findings suggest a direct link between the initial association of glycine molecules in solution and the final crystal structure. The presence of acetic acid has a significant impact on the relative abundance of building blocks corresponding to the α and γ forms in solution, and consequently on the polymorphic outcome. The results also demonstrate the utility of SAXS as a technique to directly probe molecular associations in supersaturated solutions of small organic molecules and provide insight into their role in the nucleation process.

The authors would like to thank Dr. David Gore, Dr. Alfred Y. Lee, and Dr. In Sung Lee for their help with data collection at the beam line. BioCAT is a National Institutes of Health–supported Research Center No. (RR-08630). APS is supported by the U.S. Department of Energy, Basic Energy Sciences, Office of Science, under Contract No. W-31-109-ENG-38. MRCAT is supported by the U.S. Department of Energy and its member institutions.

[1] F. Schuth, Curr. Opin. Solid State Mater. Sci. **5**, 389 (2001).
[2] V. Talanquer and D. W. Oxtoby, J. Chem. Phys. **109**, 223 (1998).
[3] P. R. ten Wolde and D. Frenkel, Science **277**, 1975 (1997).
[4] B. A. Garetz, J. Matic, and A. S. Myerson, Phys. Rev. Lett. **89**, 175501 (2002).
[5] P. G. Vekilov, Cryst. Growth Des. **4**, 671 (2004).
[6] D. Knezic, J. Zaccaro, and A. S. Myerson, J. Phys. Chem. B **108**, 10 672 (2004).
[7] S. Chattopadhyay *et al.*, Cryst. Growth Des. **5**, 523 (2005).
[8] M. Larson and J. Garside, Chem. Eng. Sci. **41**, 1285 (1986).
[9] A. S. Myerson and P. Lo, J. Cryst. Growth **99**, 1048 (1990).
[10] E. Staab *et al.*, Adv. Mater. **2**, 40 (1990).
[11] R. J. Davey *et al.*, J. Am. Chem. Soc. **119**, 1767 (1997).
[12] I. Weissbuch, M. Lahav, and L. Leiserowitz, Cryst. Growth Des. **3**, 125 (2003).
[13] R. J. Davey *et al.*, Cryst. Growth Des. **1**, 59 (2001).
[14] S. Parveen *et al.*, Chem. Commun. **12**, 1531 (2005).
[15] S. Hamad *et al.*, J. Phys. Chem. **110**, 3323 (2006).
[16] L. Yu and K. Ng, J. Pharm. Sci. **91**, 2367 (2002).
[17] G. L. Perlovich, L. K. Hansen, and A. Bauer-Brandl, J. Therm. Anal. Calorim. **66**, 699 (2001).
[18] G. Albrecht and R. B. Corey, J. Am. Chem. Soc. **61**, 1087 (1939).
[19] Y. Iitaka, Acta Crystallogr. **14**, 1 (1961).
[20] J. Ilavsky, http://www.uni.aps.anl.gov/~ilavsky/irena.html.
[21] G. Beaucage *et al.*, in *Hybrid Organic-Inorganic Composites*, edited by J. E. Mark, C. Y. Lee, and P. A. Bianconi, ACS Symposium Series Vol. 585 (American Chemical Society, Washington, DC, 1995).
[22] W. H. Orttnung, J. Phys. Chem. **67**, 1102 (1963).
[23] Z. Berkovitch-Yellin, J. Am. Chem. Soc. **107**, 8239 (1985).
[24] D. Gidalevitz *et al.*, Angew. Chem., Int. Ed. **36**, 955 (1997).
[25] C. S. Towler *et al.*, J. Am. Chem. Soc. **126**, 13347 (2004).
[26] Y. C. Chang and A. S. Myerson, AIChE J. **31**, 890 (1985).
[27] G. A. Anslow, M. L. Foster, and C. Klingler, J. Biol. Chem. **103**, 81 (1933).